



## Simultaneous 10 Gbps data and clock transmission for smart power grid application utilizing the optical fibre and VCSEL technology

H. E. Aradi, E. K. Rotich Kipnoo, F. W. Masinde, D. W. Waswa, J. Jena & T. B. Gibbon

To cite this article: H. E. Aradi, E. K. Rotich Kipnoo, F. W. Masinde, D. W. Waswa, J. Jena & T. B. Gibbon (2023) Simultaneous 10 Gbps data and clock transmission for smart power grid application utilizing the optical fibre and VCSEL technology, *Journal of Modern Optics*, 70:19-21, 1023-1030, DOI: [10.1080/09500340.2024.2380732](https://doi.org/10.1080/09500340.2024.2380732)

To link to this article: <https://doi.org/10.1080/09500340.2024.2380732>



Published online: 23 Jul 2024.



Submit your article to this journal [↗](#)



Article views: 35



View related articles [↗](#)



View Crossmark data [↗](#)



# Simultaneous 10 Gbps data and clock transmission for smart power grid application utilizing the optical fibre and VCSEL technology

H. E. Aradi<sup>a</sup>, E. K. Rotich Kipnoo<sup>a</sup>, F. W. Masinde<sup>a</sup>, D. W. Waswa<sup>b</sup>, J. Jena<sup>b</sup> and T. B. Gibbon<sup>b</sup>

<sup>a</sup>Department of Mathematics, Actuarial Science and Physical Sciences, University of Kabianga, Kericho, Kenya; <sup>b</sup>Center for Broadband Communication, Nelson Mandela University, Port Elizabeth, South Africa

## ABSTRACT

The study seeks to design a communication system for a power grid, that will ensure real-time and low-latency communication and automation between the utility and the end users. The performance characterization of the VCSEL in G.655 non-zero dispersion shifted fibre transmitting at 1550 nm is experimentally and theoretically analysed. The experiment reported the various evaluations of BER and eye diagrams using a VCSEL and a DFB laser as light sources. There was the successful achievement of 10 Gbps in 25 and 50 km for VCSEL and DFB respectively. In simultaneous data and clock transmission, 0.4 GHz and 10 Gbps over 25 km was successfully achieved using a VCSEL. The study is significant in the establishment of a pervasive communication system as the backbone of smart power grid design technology.

## ARTICLE HISTORY

Received 16 October 2023  
Accepted 2 June 2024

## KEYWORDS

VCSEL; DFB; clock signal; optical fibre; data; bit error rate

## 1. Introduction

A smart grid (SG) is a modernized electrical system in which new and more suitable models of energy production, usage and distribution will be made possible through the incorporation of a pervasive communication system and monitoring capabilities as well as autonomous and more distributed management and control functionalities into the power system [1]. Baimel et al. [2] reported that the smart grid utilizes actuators and clock systems to ensure that all grid components are under optimal control. Therefore, it must have a robust and reliable infrastructure of communication to offer communications that are secure and real-time. The infrastructure of communication should have a wide bandwidth to ascertain a high information flow rate. Thus, the utilization of optical fibre networks would be the fastest available communication type with smart grid applications since they are responsible for data transmission from one point to the next. The use of optical fibre can also facilitate the fibre to the home (FTTH) architecture by providing internet services to end users while at the same time linking the utility and the end user together in the power grid's monitoring and control system.

Measuring the signal power is a crucial aspect of signal transmission using an optical fibre. Therefore, the power of the signal transmitted along the optical fibre is

given by;

$$P_T = P_O e^{(-\alpha L)} \quad (1)$$

where  $P_T$  and  $P_O$  are the transmitted and launch powers respectively,  $\alpha$  is the attenuation coefficient and  $L$  is the fibre length in km. Traditionally, the attenuation coefficient is given by Equation (2)

$$\alpha \left( \frac{\text{dB}}{\text{km}} \right) = -10/L \text{Log}_{10}(P_I/P_O) \quad (2)$$

and is expressed in units of dB/km [2]. Calculating the attenuation coefficient provides a fraction of the scattered and absorbed energy across an optical fibre link. Optical attenuation results from both intrinsic and extrinsic effects related to the fibre. Intrinsic losses include absorption, Rayleigh scattering and dispersion at the fibre core area. Extrinsic loss mechanisms include bending losses, splicing losses, core/cladding losses and connector losses [2,3].

The vertical cavity surface emitting laser (VCSEL) is considered and together with the photodiode receiver and the optical fibre they make up the technology since the term 'technology' represents the transmitter-receiver pair. VCSELs are suitable for smart grid applications because they generate high-speed data in short-range optical communication networks [3]. In addition, they

are appealing for signal transmission due to their low consumption of power, low current, fibre coupling efficiency and fast-speed modulation at low costs of power. The VCSEL's optical power calculation is crucial in signal transmission. This can be achieved by the following equation [3].

$$P_{out} = n_i n_0 \frac{h\nu}{e} (I - I_{th}) \quad (3)$$

where  $P_{out}$  is the output power,  $n_i$  is the injection frequency,  $n_0$  the optical frequency,  $I$  is the injected current and  $I_{th}$  is the threshold current.

The power dissipated in the VCSEL is the difference between the electrical power going into the laser and the optical power coming out of the laser.

$$P_d = P_{in} - P_{out} \quad (1.4)$$

where  $P_d$  represents the dissipated power,  $P_{in}$  is the input optical power and  $P_{out}$  representing the output optical power.

High-frequency chirps, however, limit VCSEL performance in optical fibre systems and result in transmission issues at high bit rates [3,4]. These restrictions highlight the necessity to optimize and characterize optical impairments on various fibres for long-haul transmission. Wavelength division multiplexing (WDM) on the other hand increases fibre capacity. Telecommunication companies are currently utilizing both the 1310 and 1550 nm single-mode VCSELs for optical signal transmissions [5].

In a communication device comprising the optical fibre and VCSEL technology, there are two common fabrication techniques employed namely the molecular beam epitaxy (MBE) and chemical vapour deposition (CVD). In MBE VCSEL fabrication, the semiconductor layers are grown making up the VCSEL's active region. This technique provides control that is atomic scaled over the process of growth thus enabling high-quality semiconductor materials production with precise properties [6]. In CVD, material layers are deposited onto a glass substrate thereby forming the optical fibre's cladding and core layers. In VCSEL fabrication, the semiconductor layers are deposited onto a substrate thereby allowing for accurate control over the thickness and composition of the layers for the achievement of the desired electrical and optical properties [6]. These two techniques are vital in fabricating optical fibre and VCSEL based communication system with desirable characteristics such as high efficiency and minimal loss.

Long-wavelength VCSELs and other low-cost high-performance laser diodes may dominate 10 Gb/s Ethernet standards. These long-wavelength materials' narrower band gap allows lower-voltage operation [7]. The

G.655 non-zero dispersion-shifted fibre (NZDSF) has a larger core than G-652 which improves long – haul performance with low 1550 nm attenuation. It is able to pass the 25 and 50 km DWDM transmission tests because of its ability to suppress fibre non-linear effects including four-wave mixing.

Note that there is a direct proportionality between the signal's optical power density and the fibre non-linear effect that has a significant effect on the pulse shape, signal phase and the evolution of optical power, making it critical to have a proper selection of the fibre type to use for these long-haul signal transmissions [8]. Wavelength multiplexing is employed to increase the amount of data that can be transmitted over a single fibre in the array and is facilitated by the wavelength's stability and tunability [9]. Since the bit error rate (BER) is the marker of communication efficiency, it is a crucial aspect in the design of a smart power grid with reference to achieving an efficient and timely communication system.

Even though, there is still the evolution of a clear and concise smart grid definition, several characteristics still remain in control to the architectures of the smart grid architectures [10]. It is these characteristics that define the potential benefits of the smart power grid to the overall electric power system. One of the crucial characteristics is the incorporation of communication and information into every electrical generation, consumption and delivery aspect to minimize impacts on the environment, improve service and reliability, enhance markets, and improve efficiency and lower costs [11]. The clock system also plays a vital part in the smart grid technology as it is able to synchronize data transmission between the utility and the end user necessary for making electrical meter reading requests [12,13]. It helps the receiving device determine when to read the next bit or value for accurate meter readings. The paper takes the following structure: the experiment's methodology description in Section 2, the results and discussion in Section 3 and finally conclusion in Section 4.

## 2. Methodology

The experiment used the setup illustrated in Figure 1. With the utilization of a 10 Gb/s non-return to zero (NRZ) pseudo-random binary sequence (PRBS – (27-1)), a Raycan Company VCSEL lasing at 1550 nm with a – 0.9 dBm operational output power was modulated using a programmable pattern generator (PPG) through a bias tee with the modulation depth maintained at 0.3 mV.

A laser diode controller (LDC) with operating driving currents ranging from 0.5 to 9.5 mA was used to drive the VCSEL. The VCSEL was characterized to determine the output power versus bias current behaviour for

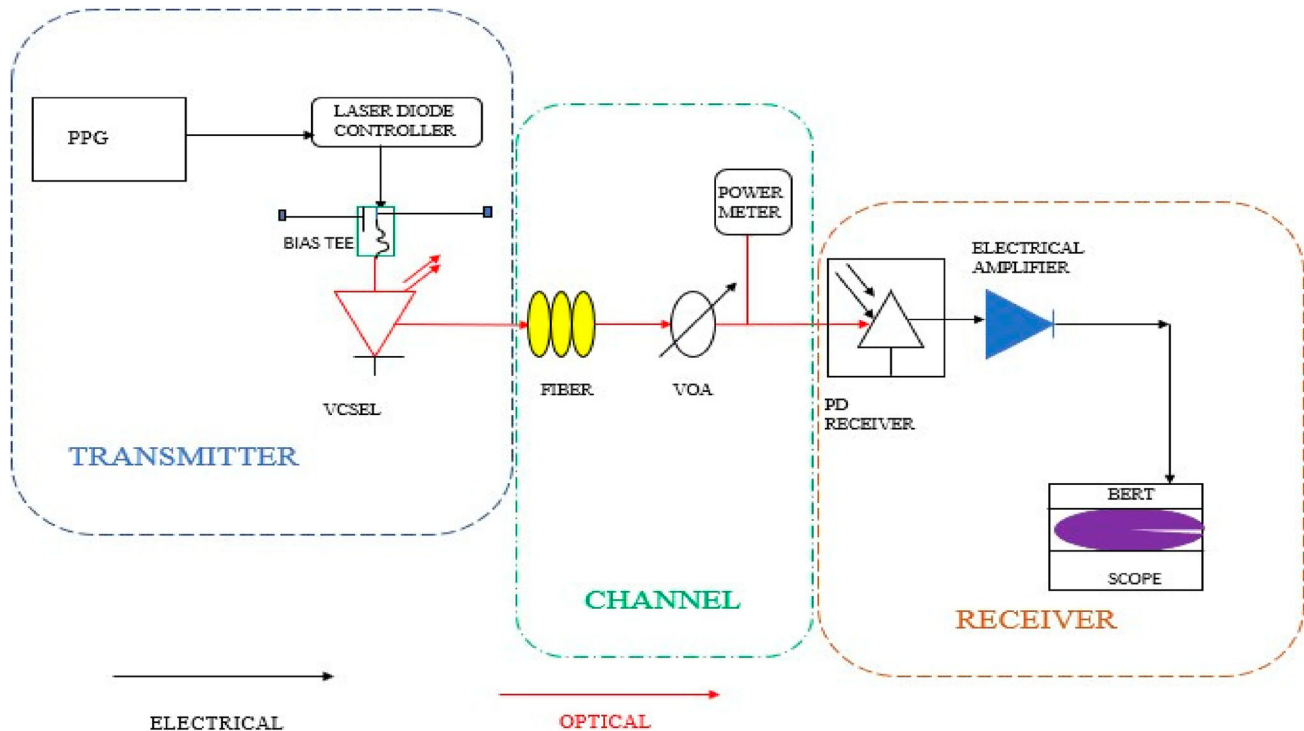


**Figure 1.** The experimental setup of a 10 Gbps directly modulated VCSEL.

both experiment and simulation. By increasing the bias currents, the wavelength tunability was also investigated. Bias currents of 2–9 mA were used to adjust the VCSEL's channel tuning. The BER was then measured for back-to-back and 25 km. This was repeated using a WDM DFB laser source at back-to-back (B2B), 25 and 50 km for comparison purposes with the VCSEL. Measurements of BER and associated eye diagrams were taken at the critical telecommunication threshold ( $10^{-9}$ ). The BER was measured by adjusting the power incident on the photo diode detector, which was achieved with the help of a variable optical attenuator (VOA). The electrical amplifier (EA) increased the voltage of the received signal to the level necessary for BER measurement. An Agilent oscilloscope was used to analyse the data from the eye diagram and wave forms. Simultaneous data and clock transmission were demonstrated by setting the frequencies on the signal generator at 0.4 and 2.5 GHz, and the input power maintained at  $-14$  dBm. VCSEL modulation voltage was tuned, and bias current ranged from 5.88 to 6.88 mA. 10 Gbps data were used to modulate a 1550 nm VCSEL. The optical carrier signal was amplitude modulated with 10 Gbps data using on-off keying (OOK). The data were transmitted across 25 km of fibre that complied with the G.655 standard using an amplitude-modulated 0.4 GHz clock signal. The clock's input power was maintained at  $-31.94$  dBm. The electrical signal generator's modulation depth was set at 0.2 mV for its RF level to generate the RF clock signal at 0.4 GHz with enough modulation.

### 3. Results and discussion

#### 3.1. VCSEL biasing

The results demonstrated the direct modulation of the VCSEL as well as the adjustment of the wavelengths through the variation of the bias current. The ability of the VCSEL to adjust both the output power and the lasing wavelength is shown in Figure 2 (a,b). From Figure 2(b) the lasing threshold was experimentally measured to be 1 mA. In simulation, on the other hand, the lasing threshold was measured at 2 mA. The low bias currents obtained from the results indicate that the VCSEL is indeed a transmitter that operates at a very low power. The experimental and simulation results shown in Figure 2(b) showed that the VCSEL's output power increased linearly with current above the threshold current. 1550 nm VCSEL saturation current was measured at 8.5 mA. As current increased above saturation, VCSEL's output power increased at a lower rate implying that its magnitude of increase per mA is less. As a result, the findings demonstrated that the VCSEL performs most effectively between threshold and saturation current levels. Through the operation of the VCSEL above its threshold level, there was the attainment of a 1548–1556 nm tunability range for a 2–9 mA current range. The results show that increasing the bias current shifted the spectrum towards higher wavelengths. Its wavelength tunability also shows that a VCSEL-based dense wavelength division multiplexing (DWDM) network with eight data

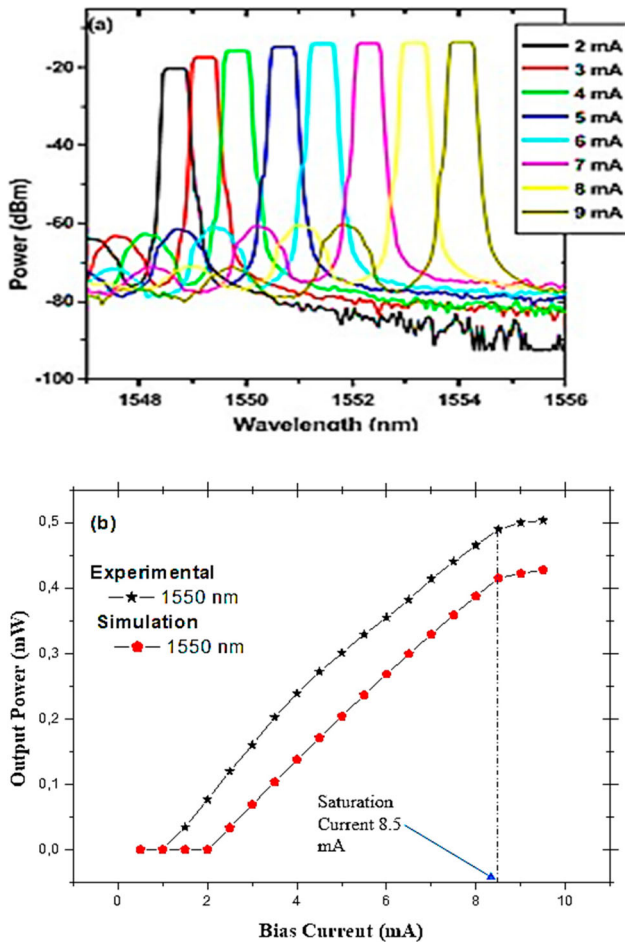


**Figure 2.** (a): VCSEL wavelength tunability/response property with tuning the bias current. (b): Experimental and simulation-based measured input current-output optical power characteristics of VCSEL at 1550 nm.

transmission channels and 50 GHz channel spacing is achievable.

### 3.2. Transmission

Using the 1550 nm VCSEL, Figure 3(a) depicts the system's performance for B2B and after 25 km. A 10 Gb/s signal's error-free sensitivity was determined experimentally using a VCSEL to be  $-17.15$  dBm in B2B. After 25 km transmission the incident power was measured at  $-14.48$  dBm indicating a 2.67 dB power penalty that was introduced by the transmission length of the fibre. The source of the power penalty was as a result of fibre dispersion which affected the optical receiver's sensitivity. In addition, since the VCSEL being a directly modulated laser is susceptible to frequency chirps, together with fibre dispersion, this degraded the sensitivity of the receiver thereby introducing a larger power penalty than in the case of the externally modulated DFB laser in Figure 3(b). In simulation however, the receiver sensitivity for B2B

was  $-15.33$  dBm and after 25 km the incident power was measured at  $-14.67$  dBm indicating a 0.66 dB transmission penalty introduced by the fibre transmission length. The simulation results verified the African Laser Center (ALC), National Research Fund (NRF), Nelson Mandela University (NMU).

In Figure 3(b), the system's performance was experimentally performed and receiver sensitivity of  $-21.58$  achieved for B2B. The respective incident powers at 25 and 50 km transmissions were recorded as  $-20.46$  and  $-20.72$  dBm respectively. The penalty of transmission after 25 km fibre was 1.12 dB. There was also the realization of more bit errors when the incident power increased with length because of the fibre's dispersion accumulation as can be seen in the waveforms. The B2B curves for simulation and experimental work varied due to factors including interference and noise in the experimental setup. These factors degraded the signal quality. Similarly, the experimental setup needed accurate measurement and calibration techniques for capturing the transmitted signals which was not the case in simulation. These variations introduced discrepancies in the curves between the experimental and simulated results. Also, factors including aging of the apparatus influenced the transmission of signals and this may not be accounted for in simulation work fully.

There was a requirement for more power at the receiver for the shorter transmission lengths in both VCSEL and DFB so as to attain the acceptable  $10^{-9}$  BER value. The introduction of the DFB laser in the experiment was so as to compare performance and sell the VCSEL technology in terms of cost and quality of service. The VCSEL was found to be a cheaper light source option for use in the experiment compared to the DFB.

The illustration in Figure 3(c) illustrates the eye diagrams and the resultant waveforms after 25 and 50 km using a DFB. It was observed that there was a further reduction in the extinction ratio of the eye diagram after 50 km fibre transmission. This shows that the longer length introduced more optical effects in the system that affected the signal quality thereby reducing the extinction ratio.

Figure 3(d) represents the obtained eye diagrams for B2B and 25 km transmission using a VCSEL. The eye openness reduced immediately after the introduction of fibre as a transmission medium. This showed that the opening of the eye and the overall extinction ratio reduced with a 25 km fibre transmission but clearly remained open in the absence of the fibre which is in essence the B2B analysis. An error free and successful transmission is characterized by a clear, wide and more open eye and therefore a dispersion compensating fibre

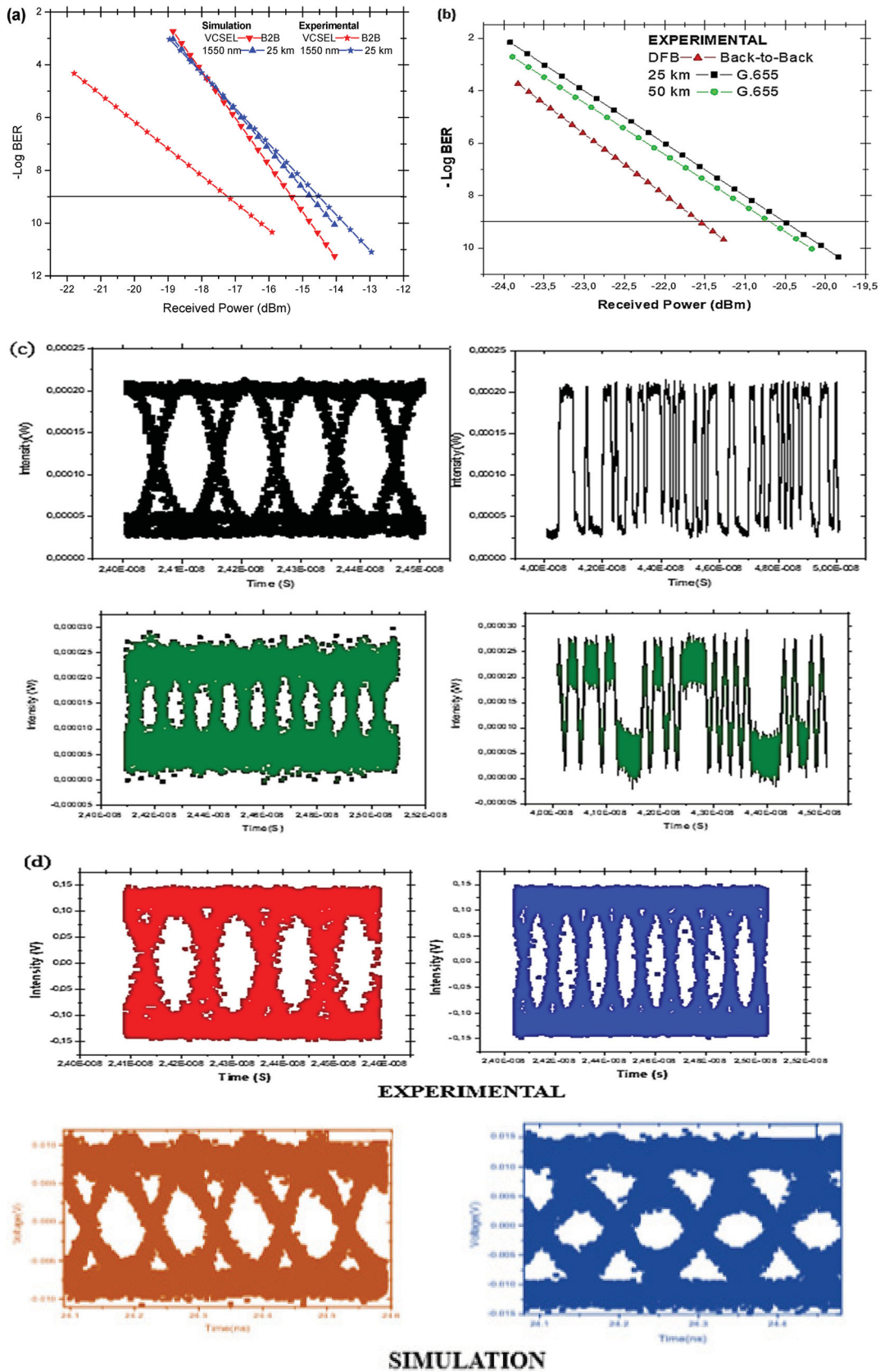


**Figure 3.** (a): Simulation and experimental plots of – Log BER curves of B2B and 25 km transmission using 10 Gbps 1550 nm VCSEL. (b): Experimental – Log BER curves for B2B, 25 and 50 km WDM DFB transmission on a G.655 fibre. (c): Eye diagrams and resultant waveforms for 25 km (black) and 50 km (green) transmission using a DFB. (d): Experimental and simulated eye diagrams for B2B (orange) and 25 km (blue) transmission (blue) using a VCSEL and G.655 fibre.

could be used at the transmitter or receiver end to minimize the dispersion. The implication of this in addition is that the receiver which was used i.e. positive intrinsic negative photodiode (PIN) was able to distinguish the transmitted bits (1 and 0) thereby reducing the bit errors. These simulation results were able to verify the experimental analysis that the extinction ratio and the intensity of the eye decrease with an increase in the transmission distance.

### 3.3. Clock and data signal transmission

Figure 4 shows the experimentally measured electrical clock signal spectrum at 0.4 GHz. It can be observed that the clock signal operated above the noise region with a power of  $-36.01$  dBm at the selected 0.4 GHz operational frequency on the signal generator.

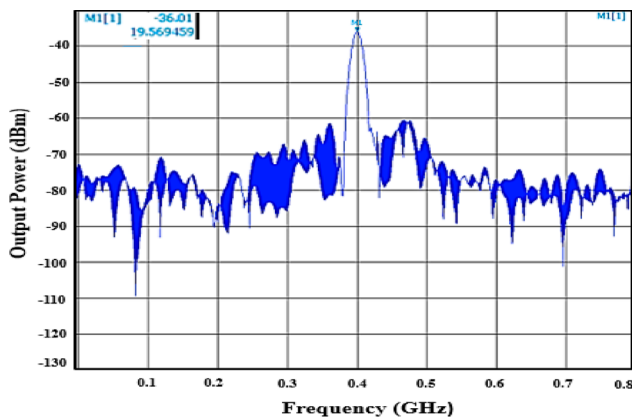


**Figure 4.** Experimentally measured electrical clock signal spectrum at 0.4 GHz.

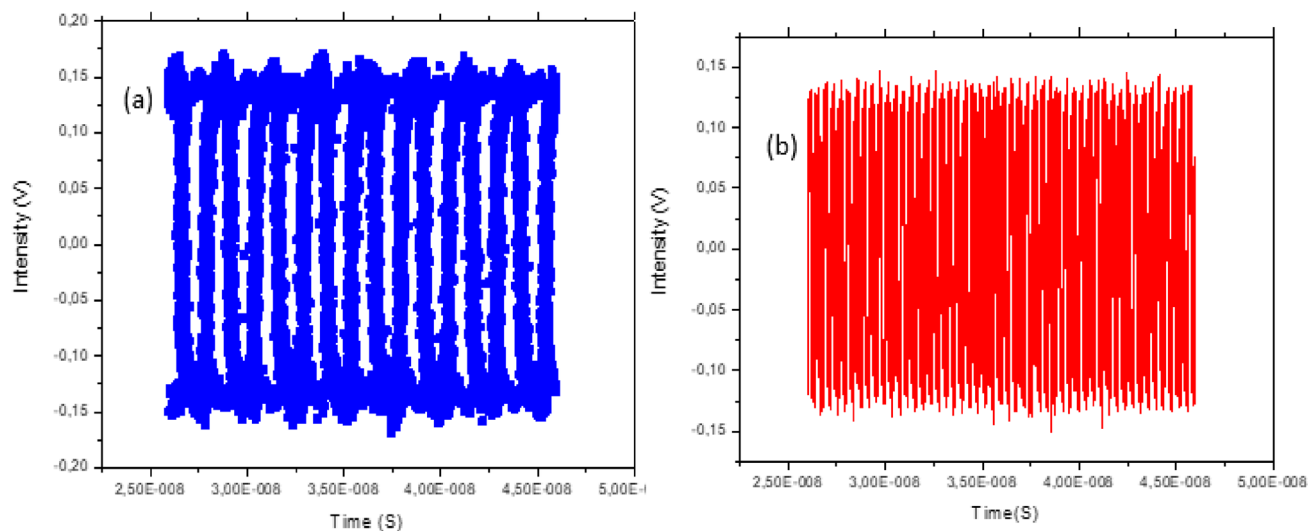


**Figure 5.** (a): A graph of electrical clock transmission 0.4 GHz transmission and (b) clock transmission 2.5 GHz.

The 0.4 GHz gave the maximum power necessary to push the strongest clock signal. In the 0.4 GHz operational frequency, the stability and performance of the clock was achieved as well as its transmission ability. The 0.4 GHz operational frequency offers a balance between efficiency and transmission power and would be used to send the request on time while reducing the power consumption during signal request transmission since the designed smart grid is based on two-way timely communication between the utility and end user.

From Figure 5(a), setting the clock signal at a lower frequency of 0.4 GHz produced a smooth waveform pattern. The superposed transmitted bits were able to form an open-eye pattern suggesting the transmitted signal's quality. On the other hand, increasing the clock frequency to 2.5 GHz produced closely packed bits and a less clear clock transmission signal. By sampling the smallest time span in Figure 6(b) it was observed that the signal intensity still varied with the same time span of propagation as in Figure 6(a) indicating that at the two frequencies, the signal travel within the same time span except for the fact that the higher frequency was not suitable for clock signal transmission. There was a different in the intensities of the two signals whereby 0.4 GHz was able to give a maximum of 0.15 V while 2.5 GHz yielded a maximum of 0.10 V. Note that two frequencies propagation time remained constant on the  $x$ -axis after sampling the bits. There was however, an increase in the time of the repetitive signal propagation by a very small range since only a small sample was taken at a small span of time.

Figure 6(a,b) represents single data and simultaneous data and clock signal transmission that was achieved by attaching the data to the clock and transmitting them at a 25 km fibre transmission at the same frequency thereafter

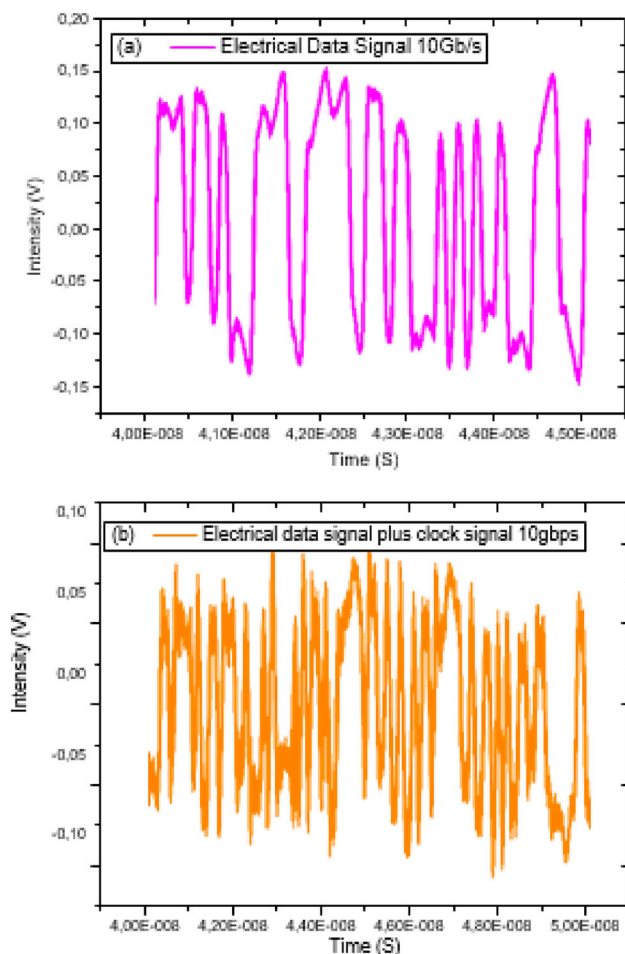


**Figure 6.** (a): A graph of 10 Gbps electrical data signal sent over 25 km fibre using a VCSEL. (b): A graph of 10 Gbps electrical data signal plus clock signal sent over 25 km using a VCSEL.

observing the two signals on the scope. Note that after the 2-signal transmission (clock and data transmission) in Figure 6(b), signal intensity decreased compared to single data transmission in (a). This was due to attenuation introduced by the fibre which affected the signal intensity. Therefore, attenuation must be minimized by introducing amplifiers and repeaters as options for far-reaching signals.

When the data-carrying optical carrier was modulated with 10 Gbps on-off keying (OOK) data and transmitted with the clock-carrier, the interference of the two interacting signals was low after fibre transmission and so the clock signal remained unaffected by a 10 Gbps optical carrier.

#### 4. Conclusion

The experiment has shown that VCSELs are best suited for transmissions up to 25 km. For longer transmission distances, the DFB laser is best suited. A 2.67 dB penalty

was realized at 25 km on a 10 Gbps VCSEL transmission and a  $-1.12$  dB transmission penalty was obtained experimentally using a DFB laser. The higher penalty using a VCSEL was due to a combination of frequency chirps and fibre dispersion that degraded the receiver sensitivity. The experiment also demonstrated wavelength tunability necessary for the creation of channel spacing between the clock and the data channels. Clock signal at 0.4 GHz over 25 km fibre transmission was also achieved. The work is significant in providing power and lighting companies with an option for achieving effective communication and real-time electrical meter request reading between end users and the utility using an affordable optical source (VCSEL). This research meets the criteria for original research work through its novelty approach. Original research involves the innovation of existing methods or exploring new avenues. This study was able to introduce a novel methodology as a criterion. The research was also able to demonstrate methodological rigour as well as adhering to scientific research standards. Finally, the research provided sufficient documentation and details for reproducibility of the findings just as the original research would. Adhering to these criteria makes the research able to contribute to the field of optical communications thereby making it possible for new developments in technology.

#### Acknowledgments

We are grateful to the Nelson Mandela University (Centre for Broadband Communication) and the African Laser Centre (ALC) through a collaboration with the University of Kabianga for the research visit and funding that aided the experiment.

#### Disclosure statement

No potential conflict of interest was reported by the author(s).

#### Funding

This work was supported by African Laser Centre, Council for Scientific and Industrial Research; Nelson Mandela University.

#### References

- [1] Smartgrid.gov. Smart Grid: The Smart Grid | Smart-Grid.gov. Retrieved 25 March 2023, 2021. [https://www.smartgrid.gov/the\\_smart\\_grid/smart\\_grid.html](https://www.smartgrid.gov/the_smart_grid/smart_grid.html).
- [2] Baimel D, Tapuchi S, Baimel N. Smart grid communication technologies- overview, research challenges and opportunities. *Int Symp Power Electron Elect Drives Autom Motion (SPEEDAM)*. **2016**: 116–120. doi:10.1109/SPEEDAM.2016.7526014
- [3] Iga K. Surface-emitting laser-its birth and generation of new optoelectronics field. *IEEE J Sel Top Quan Elec*. **2000**;6(6):1201–1215. doi:10.1109/2944.902168



- [4] Soderberg E, Gustavsson JS, Modh P, et al. Suppression of higher order transverse and oxide modes in 1.3- $\mu\text{m}$  InGaAs VCSELs by an inverted surface relief. *IEEE Photon Technol Lett.* **2007**;19(5):327–329. doi:10.1109/LPT.2007.891631
- [5] Kipnoo R, Kiboi Boiyo EK, Isoe D, et al. Demonstration of Raman-based, dispersion-managed VCSEL technology for fibre-to-the-hut application. *Opt Fibre Tech.* **2017**;34:1–5. doi:10.1016/j.yofte.2016.12.001
- [6] Asahi H, Horikoshi Y. (Eds.). *Molecular beam epitaxy: materials and applications for electronics and optoelectronics.* John Wiley & Sons; 2019. <https://ieeexplore.ieee.org/servlet/opac?bknumber=8653932>
- [7] Gibbon TB, Prince K, Pham T, et al. VCSEL transmission at 10Gb/s for 20km single mode fiber WDM-PON without dispersion compensation or injection locking. *Optical Fiber Technol.* **2011**;17(1):41–45. doi:10.1016/j.yofte.2010.10.003
- [8] Ellis AD, McCarthy ME, Al Khateeb M, et al. Performance limits in optical communications due to fiber nonlinearity. *Adv Opt Phot.* **2017**;9(3):429–503. doi:10.1364/AOP.9.000429
- [9] Li C, Bai R, Shafik A, et al. A ring-resonator based silicon photonics transceiver with bias-based wavelength stabilization and adaptive-power-sensitivity receiver. In *2013 IEEE International Solid-State Circuits Conference Digest of Technical Papers*; 2013. p. 124–125. IEEE.
- [10] Sayed K, Gabbar HA. SCADA and smart energy grid control automation. In *Smart energy grid engineering.* Elsevier; 2017. p. 481–514. doi:10.1016/B978-0-12-805343-0.00018-8
- [11] Kemal M, Olsen R. Analysis of timing requirements for data aggregation and control in smart grids. In *2014 22nd Telecommunications Forum Telfor (TELFOR).* IEEE; 2014. p. 162–165.
- [12] Isoe, G. M., Wassin, S., Gamatham, R. R. G., et al. Simultaneous 10 Gbps data and polarization-based pulse-per-second clock transmission using a single VCSEL for high-speed optical fibre access networks. In *Optical Metro Networks and Short-Haul Systems IX*; 2017. p. 87–98 (Vol. 10129). SPIE.
- [13] Karembere R, Nfanyana K, Gibbon T. Simultaneous transmission of clock and data signals in photonic-assisted WDM passive optical networks. *JOSA B.* **2021**;38(3): 914–921. doi:10.1364/JOSAB.413907